San Jose State University | ME 201 Master's Thesis Proposal | 2021 August 20 2021

1.0 Name [redacted]

2.0 Title

Electrochemomechanical Effects of Cyclic Compression on a Composite Polymer Electrolyte for Lithium-Ion Batteries

3.0 Background

The increasing demand for battery power has led to the development of several material systems for lithium-ion batteries. Composite polymer electrolytes (CPE) are safer than the more common organic liquid electrolytes due to their decreased flammability and resistance to overheating. However, the liquid electrolytes have much better ionic conductivity than the CPE. Ceramic materials such as $Li_{6.4}La_3Zr_{1.4}Ta_{0.6}O_{12}$ (LLZTO) or $Li_{6.4}La_3Zr_{1.4}O_{12}$ (LLZO) are some of the more promising filler materials for enhancing ionic conductivity in the CPE [1]. Very little is known about the mechanics of these recent polymer electrolytes and how they respond to the internal stresses caused by volumetric changes in the battery.

3.1 Volume Change of Electrolytes During the Charging Cycle

There are two prevalent methods for measuring the electrochemical expansion of the CPE. One method is to limit the force applied to the battery and measure the displacement and the other is to limit the displacement of the battery and measure the force that it exerts. Koerver et al. took the latter approach, using a series of springs to create a model for the expansion force of the battery. Koerver was able to model an ideal representation using two springs in a series, where the lengths of the springs were proportional to the fractional volumes of the different phases of the cathode. This combination of springs produced an easier way to calculate the effective Young's modulus of the system [2]. A simpler and more straightforward way to measure the volume change is to apply a constant load to the battery and measure the displacement. Lee et al. placed a battery between two parallel plates before applying a 300 g load. They then used a thickness gauge and an automatic data logger to measure the displacement [3]. Barker used a linear voltage displacement transducer with their thickness

gauge to get a finer resolution measurement of the dimensional changes than the automatic data logger from Lee's research [4].

3.2 Stress-Strain Testing of Polymer Electrolytes

Another approach for studying polymer electrolytes is through stress-strain testing. Kelly et al. investigated the ionic conductivity of polyethylene oxide (PEO) electrolytes and how the conductivity fluctuates under tensile strain. Their main focus was the functionality of battery electrolytes when stretched. This experiment used impedance spectroscopy, which sends an excitation signal through the material to measure the resistance and capacitance. The main takeaways from this research are that the more the electrolyte is stretched, the lower the impedance, leading to an increase in conductivity. Kelly found that the Coefficient of Strain Dependent Ion Conductivity Enhancement (CSDICE) remained similar regardless of the plane of measurement of the CPE. This suggests that CSDICE is an isotropic property and relates more with how the polymer chains react to each other rather than which direction they are stretched [5]. Lee et al. ran compressive tests on polydimethylsiloxane (PDMS) elastomer. They added a curing agent to the PDMS and observed how the mechanical properties changed as the concentration of the curing agent increased. This group ran two different tests, a compression test to failure and another cyclic compression test in which they alternated between 0% strain and 20% strain for 100 cycles. The viscoelastic response they observed exhibited some hysteresis, which represented dissipated energy while the sample was under compression. However, the amount of hysteresis decreased as the compressive cycling on the battery increased. Another effect of the cyclic compression was strain hardening which they attributed to increases in both peak stress and elastic modulus as the battery was cycled [6]. Sauerteig et al. took the approach of using electrochemical impedance spectroscopy to measure the stress-strain behavior of their 10 A·h capacity hybrid electric vehicle cell. They ran the spectroscopy by creating 10 mV perturbations and cycling the frequency from 100 kHz to 1 Hz at a rate of 10 frequency points per decade. Their results showed that the stress-strain curve was nonlinear, which was consistent with other porous polymers. However, Sauerteig observed some stiffening in the electrolyte, found by taking the derivative of the compression curve. This stiffening was attributed to electrolyte decomposition products that were created from the compressive cycling [7].

3.3 Effects of Thermal Expansion on Battery Cells

Looking at the thermal expansion of batteries, Oh et al. was able to capture information by running two similar experiments. In the first experiment, they measured the thermal swelling of the cell from 5 ℃ to 45 ℃ to attain the total thermal expansion with the surrounding fixture and sensor of their system included. In the second experiment, Oh replaced the cell with an aluminum block of the same dimensions. Since the coefficient of thermal expansion for the aluminum was known, they were able to separate the two thermal expansion values and find the excess expansion of the fixture and sensor. They were then able to use those values to isolate the expansion of the cell from the first experiment [8]. In a separate study, Oh et al. ran a test to determine the thermal expansion of an electric vehicle battery cell. This time, Oh charged the cell in an insulated environment where the cell expansion could be attributed to both thermal and electrochemical expansion. Subsequently, they ran the same experiment in a thermal chamber that could regulate the temperature and counteract the thermal expansion. By comparing the results from both experiments, they were able to find a 1.5% difference in expansion at low discharge rates. This difference increased as the battery approached higher discharge rates. Furthermore, the expansion was not uniform, with the center of the cell expanding more than the edges [9]. Heinz et al. studied Na-$NiCl_2$ cells under high temperatures. These cells performed well because the sodium melted at higher temperatures, surrounding the $NiCl_2$ in a molten electrolyte base that did not have a major effect on the charging functionality. However, the concern for Heinz was that the pressure changes resulting from the high-temperature molten sodium created stresses that were detrimental to the cell. By testing the pressure changes in multiple cell designs, Heinz found that hollow tubular cells fared better against the increased stress than conventional planar cells [10].

3.4 Optical Imaging of Particles in Battery Electrolytes

Optical imaging can be utilized to observe the particles within the battery cell. Jones et al. used digital image correlation to measure the strains and cracks that arose in Li-ion batteries as they were charged. Jones took multiple images of the electrode surface via an in situ image capture device. They then used the digital image correlation software to measure changes in strain throughout the cycle. Jones found that the cell expanded by 1.41% during lithiation and contracted by 1.33% during delithiation [11]. Xie et al. created an optical acquisition system

using a telecentric lens to monitor the deformation of their silicon electrode in real time. With the use of their system, Xie was able to find that the compressive stress of the composite increased as lithium particles were added to the silicon electrode. They also discovered that softening the silicon electrode could alleviate stress from lithium particles [12]. Rees et al. used magnetic resonance imaging to observe the growth of sodium dendrites in solid-state batteries. Using this imaging technology, dendrites with a skin depth of 11 μm were found. These dendrites lead to cell failure because of how they penetrate the cell and cause short circuits. Therefore the magnetic resonance imaging was extremely useful in observing the dendrite growth so that new solutions could be engineered to prevent such failures [13].

3.5 Effects of Mechanical Compression on Electrical Conductivity

Looking closer at the effects that mechanical compression has on electrical conductivity, Bouziane et al. conducted a study on the electrical contact resistance between different layers of fuel cells. They measured the contact resistance of various gas diffusion layers under cyclic compression using the Transmission Line Method, a method used to find the electrical contact resistance between a metal and a semiconductor. For all seven of the tested gas diffusion layers, Bouziane found a nonlinear decrease in the specific electrical contact resistance as the applied pressure increased. They hypothesized that the stress improved the contact between the gas diffusion layers by increasing the contact surface and decreasing the porosity. This led to the decrease in measured resistance and the improvement in conductivity [14]. Mason et al. conducted a similar experiment measuring the effects of compression on electrical conductivity in fuel cells. They used electrochemical impedance spectroscopy to differentiate between the contact resistance and the mass transport resistance of the fuel cell. Mason found similar results to Bouziane in which the electrical contact resistance decreased as the fuel cell was compressed. However, the mass transport resistance exhibited an opposing effect, in which the resistance increased as the fuel cells were compressed. This can be attributed to permanent tearing and cracking in the fuel cell due to the applied stress. These competing resistivities led Mason et al. to conclude that there was an optimal compression limit where both the contact resistance and the mass transport resistance were minimized [15].

The intellectual merit and significance of this project is that while the addition of LLZTO particles is known to increase the ionic conductivity of electrolytes, the long term mechanical

effects of these particles is less known. Whether it be, microcracking, fatigue hardening, or dendrite growth, studying the mechanical properties of the CPE will be crucial in developing solid-state electrolyte technology.

4.0 Objective

The hypothesis of this investigation is that the addition of ion conducting ceramic particles to polymer electrolytes is capable of reducing the impedance of the composite electrolyte when subjected to cyclic compression. The reasoning is that compression can remove undulations and irregularities in the electrolyte, providing a homogenizing effect and reducing the impedance. A quantitative evaluation metric for modeling is the closeness of fit between experimental relaxation data and a generalized Maxwell model for viscoelasticity. The generalized Maxwell model contains Maxwell elements that can be added or removed based on any complications with the polymer [16]. Two important performance metrics are the impedance of composite electrolytes and the long-cycle stability of charge capacity (i.e., very slow degradation rate with respect to number of charge and discharge cycles.). It is envisioned that quantitative results from this work will help to determine how to reduce impedance and prolong charge capacity.

The process of adding ceramic particles to polymer electrolytes can introduce undulations and irregularities to the electrolytes. These undulations can affect the apparent modulus of the electrolyte, with the inconsistencies of the material leading to a lower modulus than if the polymer were completely homogenous. Therefore, if the compressive cycling process can improve the homogeneity of the electrolytes, the apparent modulus will approach values closer to the native modulus of the CPE.

5.0 Methodology

Mechanical-only tests will be conducted using an ElectroPuls E1000 dynamic testing system (Instron, Norwood, Massachusetts, USA) outfitted with a 2 kN load cell. All tests will be conducted at room temperature without environmental humidity control. The gauge thickness of each individual test specimen will be measured between glass slides using a digital micrometer with 1 μm resolution. All tests will be conducted on three types of test specimens: No LLZTO, 5 μm LLZTO, and 500 nm LLZTO.

The main resources needed for this thesis include, access to the Instron ElectroPuls E1000 to run precise tests on the specimen, access to the Instron WaveMatrix software in order to program the ElectroPuls to perform the necessary movements, raw materials (PEO and LLZTO), equipment, and the training needed to prepare the battery electrolytes. The materials, equipment, and manufacturing will be provided by [redacted]

The most significant risk to this experiment would be that if the specimens are too thin, they might tear while being separated from the attached film, compromising the repeatability of the experiment. The contingency for this would be to try multiple thicknesses to find one that is both easy to manufacture and easily separated. Furthermore, extra electrolyte films could be produced so that if some were to tear then they could be easily replaced during testing. It must be noted that this contingency would place a greater burden and responsibility on the fabrication and fabricator of the specimen. However, recent communications suggest that fabricating higher quantities of test specimens is not overly taxing or time consuming. Another major risk would involve losing collaboration for the manufacturing and materials of the CPE. To mitigate this, I could undergo training or shadow [redacted] to be able to manufacture the electrolytes myself in the case that they are unavailable.

5.1 Stress-Strain

The first type of experiment involves preconditioning through five cycles of compression and unloading. The specimens are compressed by 20% strain at a rate of 1 Hz. The data acquisition system records load and position data, from which the stress can be calculated by dividing the load by cross-sectional area. The strain is calculated by taking the positioning data and subtracting the setpoint value to find the local displacement, which is divided by the specific gauge thickness of each individual specimen to determine strain. The stress-strain curves are also used to find appropriate magnitudes of preload and peak stress for the subsequent stress relaxation and compressive cycling experiments which will use fresh, but identically prepared specimens.

5.2 Stress Relaxation

Stress relaxation experiments consist of compressing each specimen to a prescribed peak stress and holding the position fixed while the material relaxes. More specifically, the test begins by ramping up to the displacement corresponding to a prescribed initial peak stress. The initial descent onto each test specimen is completed gradually over approximately ten seconds to prevent dynamic overshoot. Once the prescribed initial peak stress is reached, the compression grip is held at the same fixed position for 600 s. The magnitude of the initial peak stress (12 kPa ± 2 kPa) is selected based on preliminary trials to be in a consistent range of the maximum expected stress at 15% strain for all three types of test specimens.

5.3 Cyclic Compression

Similar to the stress relaxation procedure, the magnitude of the head displacement is selected to ensure a consistent initial peak stress for all three types of specimens (12 kPa ± 2 kPa). After a first gradual approach to the initial peak stress, the instrument completes 500 cycles at a rate of 3 Hz. This driving input to cyclic loading follows a trapezoidal waveform, in which the amplitude is determined by the difference between the preload displacement and the peak stress displacement. For each of the five hundred cycles, the upper compression head starts at the preload setpoint before ramping to the prescribed amplitude over the course of one second. The compression head then holds at the peak position for 0.5 s before ramping back down to the preload displacement and holding for 0.5 s again.

5.4 Surface Topography

In order to discern the effect of compressive cycling on the undulations and pores within the CPE, there must be a way to quantify those irregularities. Therefore, the next portion of the experiments will include taking scanning electron microscopy (SEM) images of the specimens before and after the cyclic compression tests. The purpose of these will be to distinguish any differences on a magnified level and identify the size and location of pores before and after the cycling process. The scanning electron microscopy will be performed in the Materials Characterization and Metrology Center (at San Jose State University), where preliminary images have been taken for similar test specimens. The before and after cycling SEM images will be taken for all three types of LLZTO specimen. This will provide additional information on

whether the size of the LLZTO particles added has any effect on the pores and undulations seen in the SEM images. In addition to the SEM images, optical profilometry will be performed on the specimens to provide a measurement of the undulation sizes from before and after cycling. Optical profilometry will be performed on a Wyko NT9100. (Bruker Corp., Billerica, MA).

5.5 Electrochemical Impedance Spectroscopy

Similar to the scanning electron microscopy, electrochemical impedance spectroscopy (EIS) will be done on the composite electrolytes before and after the cyclic compression process. The impedance spectroscopy is done by connecting the electrolytes to a Gamry Instruments Interface 1010E in order to measure the impedance of the CPEs and whether they improve through the cyclic compression process. In addition to the commercial (Instron) test system for mechanical-only testing, we have also designed and fabricated a smaller open-frame apparatus that facilitates simultaneous measurement of displacement, force, and impedance. A brief description is included in the Preliminary Work section below, and early stages of the Fall 2021 semester will involve testing and calibrating this custom apparatus.

6.0 Deliverables

The first deliverable will be a stress-strain curve showing hysteresis of the electrolyte. This plot will have strain on the x-axis and stress on the y-axis. Task 1.1 consists of preparing three sets of PEO electrolytes: without the LLZTO particles, with 5 μm LLZTO particles, and with 500 nm LLZTO particles. Task 1.2 will be conducting a resolution test on the Instron ElectroPuls E1000 by running it in tandem with the more accurate displacement sensor of the Keyence GT2. Task 1.3 will entail performing stress-strain tests on multiple replicates and organizing the data in a stress-strain curve plot.

The second deliverable will be the scanning electron microscopy images of the CPE from before and after cycling. The supporting tasks for this deliverable include Task 2.1, taking magnified SEM images before the specimens are cycled, and Task 2.2, taking magnified SEM images after the specimens have been cycled. These tasks will be closely linked to the third deliverable as the latter of the scanning electron microscopy images needs to take place after the fatigue cycling test.

The third deliverable will be a plot highlighting the cyclic compression of the CPE. This plot will include cycles on the x-axis and stress on the y-axis. Task 3.1 will be conducting preliminary compression tests and determining the necessary strain placed on the test specimen in order to see a compression limit. Task 3.2 consists of running cyclic compression tests on the specimen with different sizes of LLZTO particles to receive data on the viscoelastic response of the polymer electrolytes. These tests will be run for 500 cycles, compressing the material at the strain specified by Task 3.1. Task 3.3 will involve digesting the data and plotting it on a cycles vs. stress plot in order to determine the extent of fatigue hardening involved.

The fourth and most summative deliverable will be a set of Nyquist plots (i.e., imaginary vs. real components of impedance) that compare impedance spectra for composite electrolytes that have been subjected to cyclic compression or not. This deliverable will be closely related to Task 3.2 as the impedance must be measured before and after the cyclic compression tests. Task 4.1 consists of taking the EIS measurements of the electrolytes before the cyclic compression test. Task 4.2 involves taking the EIS measurements of the electrolytes after they have been cycled. Task 4.3 consists of digesting and summarizing the data into a set of Nyquist plots to compare the impedance spectra for the CPEs

7.0 Timeline

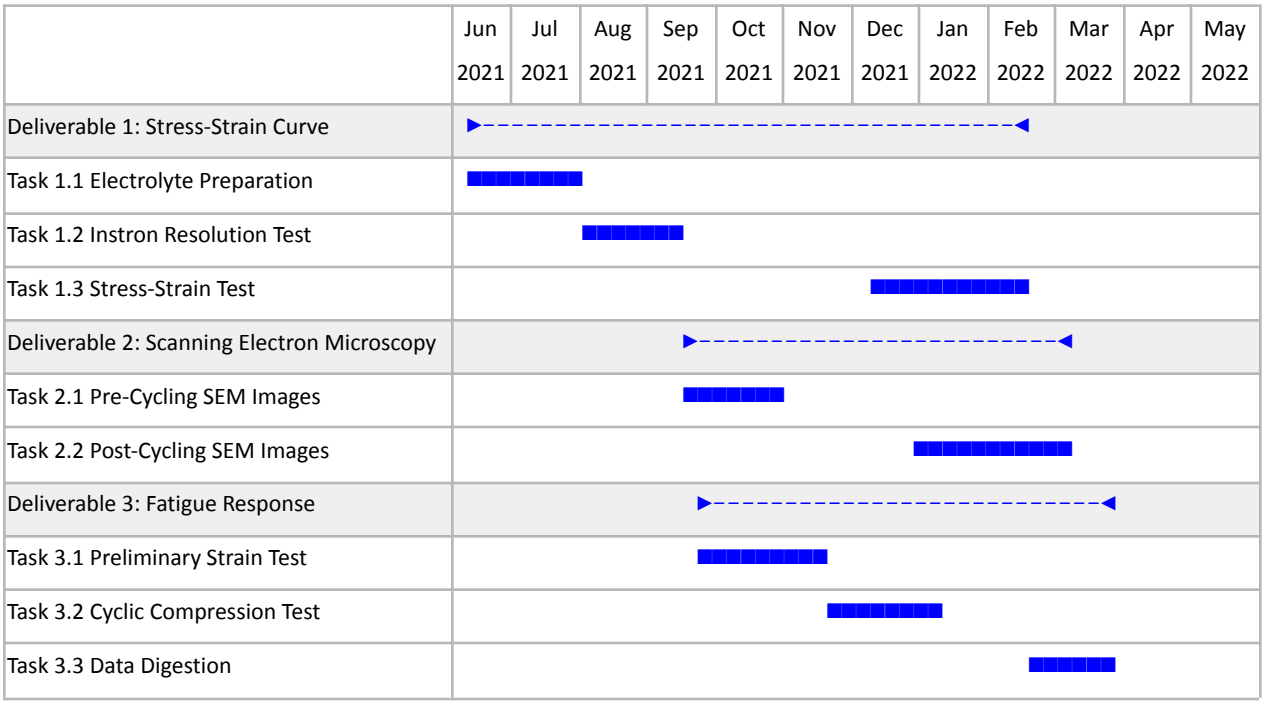

Deliverable 4: Electrochemical Impedance Spectroscopy	
Task 4.1 Pre-Cycling EIS Measurements	
Task 4.2 Post-Cycling EIS Measurements	
Task 4.3 Comparative Nyquist Plots	

8.0 Preliminary Work

The preliminary work being presented in the report consists of four accomplishments: (1) a stress relaxation plot to estimate the long term relaxation times of the specimen, (2) a cyclic stress-strain curve to determine the necessary strain to be placed on the specimen and the compression limit, (3) a test method that can use the software to communicate with the ElectroPuls E1000, and (4) prototyping of modular apparatus that has been designed for measuring force, displacement, and impedance simultaneously. All four of these contributed to providing information and setting up the experiments proposed in the methodology above. The testing for both the stress relaxation plot and the stress-strain curve was done on a PEO electrolyte without any added LLZTO which was provided by the Energy Materials Laboratory.

8.1 Stress Relaxation Plot

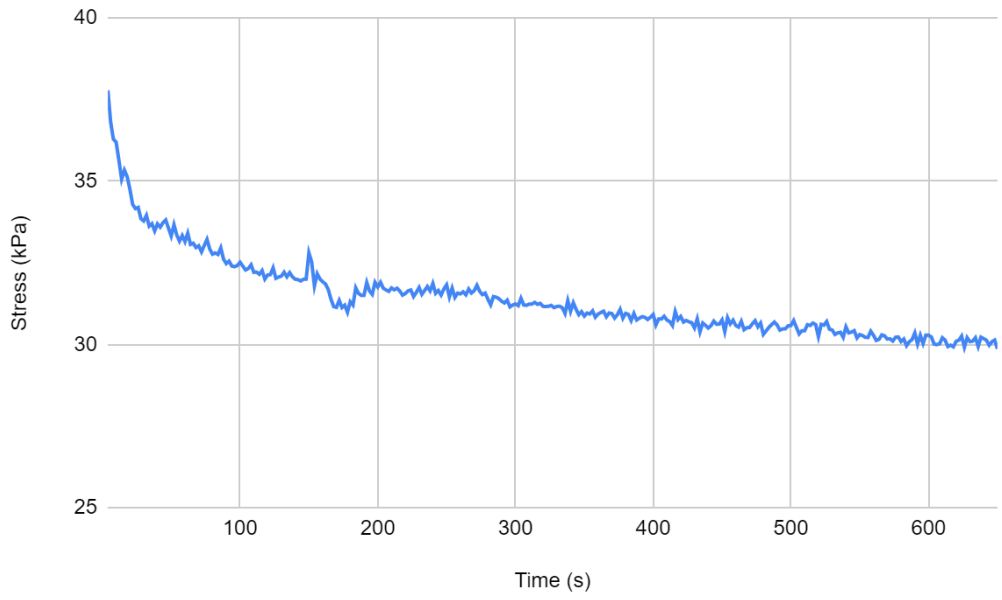

Figure 1. Stress relaxation plot. Shows the stress relaxation of a PEO specimen. The stress peaks at a value of 38 kPa but as the polymer relaxes, the stress decreases to 30 kPa at 600 seconds.

The stress relaxation plot consisted of compressing a PEO specimen to a prescribed strain amount and holding at that displacement for an extended period of time. This helped to determine how long the polymer took to relax and that time estimate was used as a base point for the final experiment to ensure that none of the critical relaxation data was cut off by too short of a relaxation time. As seen in Figure 1, the specimen was relaxed by the 600 second mark. Therefore, a good time estimate would be ten minutes for the relaxation of the PEO electrolytes.

8.2 Stress-Strain Curve

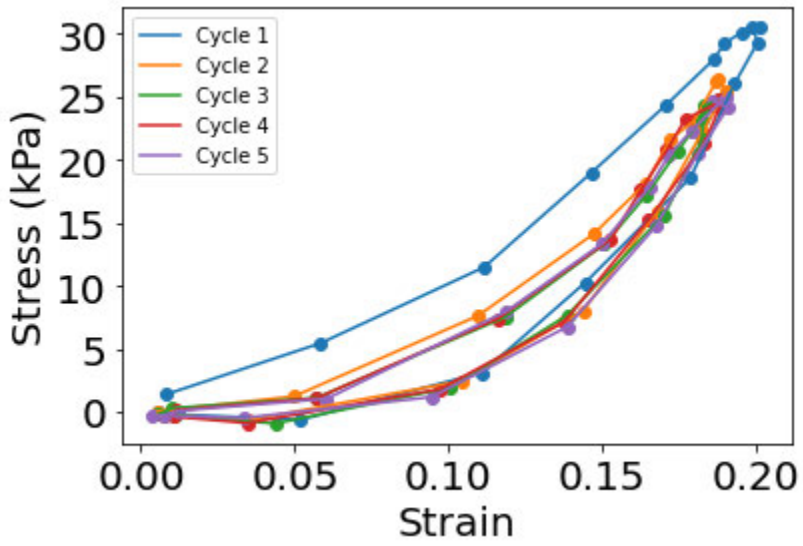

Figure 2. Cyclic stress-strain curve. Shows the cyclic stress-strain curve plotted over five cycles of compression. The maximum stress on this curve is approximately 30 kPa which converts to a compression limit of 2.1 N.

The cyclic stress-strain curve also involved compressing the PEO specimen to a prescribed strain. However, instead of holding the compression for an extended amount of time, this process consisted of oscillating through this compression and decompression for five cycles. Since each of the specimens were extremely thin, at about 100 μm thick, it was difficult to visually distinguish the point at which the compression grips were in contact with the specimen.

Therefore, 1% of the maximum stress was considered to be the preload, or the zero value, for other tests moving forward. Based on Figure 2, the preload was the amount of force needed to produce 0.3 kPa of stress. This preload ensured that the compression head was in contact with the specimen without exerting too much force on the electrolyte before the experiment began.

8.3 Test Method

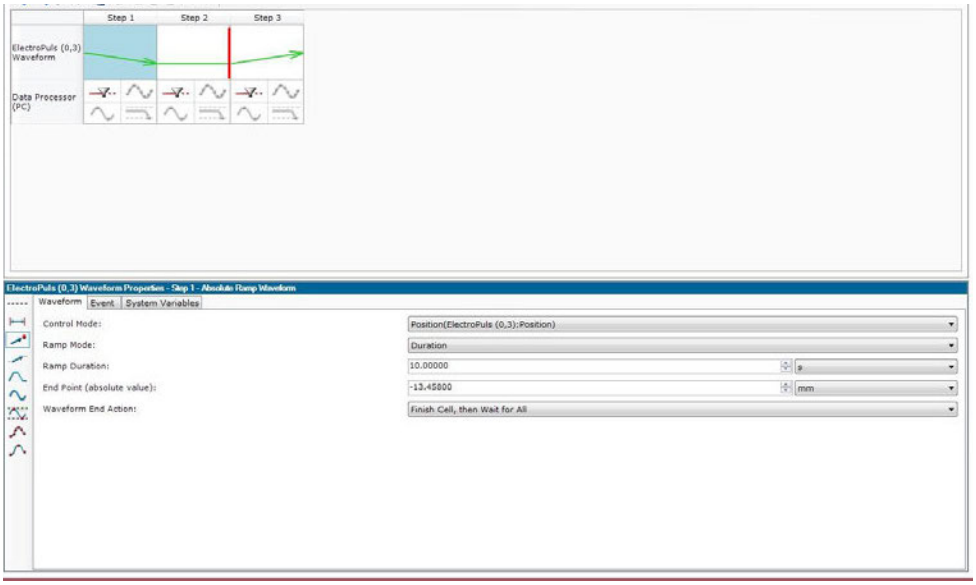

Figure 3. Stress relaxation test method. Shows a screenshot of the Instron WaveMatrix software for the stress relaxation test method.

Finally, a test method was created from the Instron WaveMatrix software. This consisted of putting all the previous data such as the relaxation time and preload into the software and arranging the tests sequentially to prepare them for testing. The test method also contained ancillary information such as the data acquisition rate and the necessary outputs. The test method in Figure 3 involved ramping down the compression grip to the adjustable end point. This end point was set to the displacement value at which the peak stress determined from the preliminary stress-strain curve occurred. To continue with the data from Figure 2, the displacement value would correspond to the previously discovered 2.1 N compression limit. The compression head was then held there for 650 seconds to encompass the 600 second time estimate taken from the preliminary stress relaxation plot.

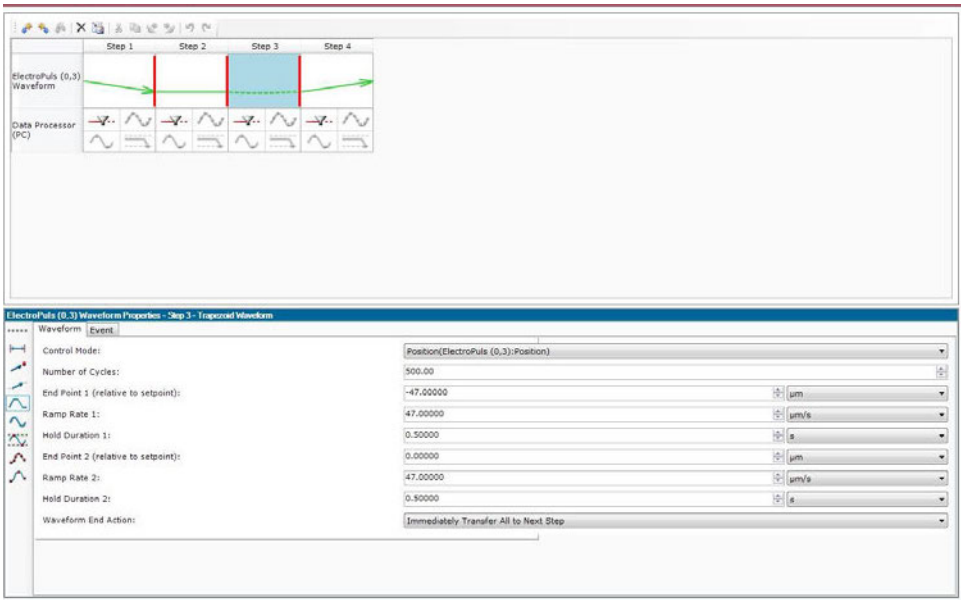

Figure 4. Fatigue cycling test method. Shows a screenshot of the Instron WaveMatrix software for the fatigue cycling test method.

The test method in Figure 4 started by ramping down to the preload "zero" point determined by the preliminary stress-strain curve. It then used a trapezoidal wave to cycle through the compression cycle 500 times. Initially, a sine wave was used for this process but there was a period where the sine wave was above the x-axis that the compression grip would lift off the specimen. Through trial and error, the trapezoidal wave was found to fix this issue. Therefore in the test method, the Instron was told to compress the specimen by a specified displacement. It then held there for half a second before coming back up to the zero point and holding for half a second again. The test method for the stress-strain testing was similar to this one with the 500 cycles adjusted down to five cycles.

8.4 Design and Prototyping of Apparatus for Simultaneous Electrochemomechanical Testing

Figure 5. CAD model of simultaneous electrochemomechanical testing apparatus. Left side shows an exploded view with the relevant parts labeled. Right side shows a compact overview of how the apparatus looks when fully assembled.

The simultaneous electrochemical testing apparatus modeled in Figure 5 was designed to measure multiple aspects of the electrolytes at the same time. The electrolyte is placed in the center with a load cell below it to measure the force of the expanding CPE. The Keyence GT2 digital contact sensor is placed through a tapped hole at the top to measure the displacement of the electrolyte as it expands and contracts. Alligator clip contacts are placed on either end of the apparatus to provide an electrical connection and measure the impedance of the electrolyte while charging and discharging. The goal of this apparatus is to combine and streamline the different experiments of this thesis in order to cut down on data loss due to specimen transportation and storage between experiments.

9.0 References

[1] Wang, C., Fu, K., Kammampata, S. P., McOwen, D. W., Samson, A. J., Zhang, L., Hitz, G. T., Nolan, A. M., Wachsman, E. D., Mo, Y., Thangadurai, V., and Hu, L., 2020, “Garnet-Type Solid-State Electrolytes: Materials, Interfaces, and Batteries,” Chem. Rev., 120(10), pp. 4257–4300.

[2] Koerver, R., Zhang, W., Biasi, L. d., 2018, "Chemo-Mechanical Expansion of Lithium Electrode Materials – on the Route to Mechanically Optimized all-Solid-State Batteries," Energy & Environmental Science, 11(8), pp. 2142-2158.

[3] Lee, J. H., Lee, H. M., and Ahn, S., 2003, "Battery Dimensional Changes Occurring during Charge/Discharge Cycles—thin Rectangular Lithium Ion and Polymer Cells," Journal of Power Sources, 119-121, pp. 833-837.

[4] Barker, J., 1999, "In-Situ Measurement of the Thickness Changes Associated with Cycling of Prismatic Lithium Ion Batteries Based on LiMn2O4 and LiCoO2," Electrochimica Acta, 45(1), pp. 235-242.

[5] Kelly, T., Ghadi, B. M., Berg, S., 2016, "In Situ Study of Strain-Dependent Ion Conductivity of Stretchable Polyethylene Oxide Electrolyte," Scientific Reports, 6(1), pp. 20128.

[6] Lee, W. S., Yeo, K. S., Andriyana, A., 2016, "Effect of Cyclic Compression and Curing Agent Concentration on the Stabilization of Mechanical Properties of PDMS Elastomer," Materials & Design, 96, pp. 470-475.

[7] Sauerteig, D., Hanselmann, N., Arzberger, A., 2018, "Electrochemical-Mechanical Coupled Modeling and Parameterization of Swelling and Ionic Transport in Lithium-Ion Batteries," Journal of Power Sources, 378, pp. 235-247.

[8] Oh, K., and Epureanu, B. I., 2016, "A Novel Thermal Swelling Model for a Rechargeable Lithium-Ion Battery Cell," Journal of Power Sources, 303(C), pp. 86-96.

[9] Oh, K., Siegel, J. B., Secondo, L., 2014, "Rate Dependence of Swelling in Lithium-Ion Cells," Journal of Power Sources, 267, pp. 197-202.

[10] Heinz, M. V. F., Graeber, G., Landmann, D., 2020, "Pressure Management and Cell Design in Solid-Electrolyte Batteries, at the Example of a Sodium-Nickel Chloride Battery," Journal of Power Sources, 465, pp. 228268.

[11] Jones, E., Silberstein, M., White, S., 2014, "In Situ Measurements of Strains in Composite Battery Electrodes during Electrochemical Cycling," Experimental Mechanics, 54(6) pp. 971-985.

[12] Xie, H., Zhang, Q., Song, H., 2017, "Modeling and in Situ Characterization of Lithiation-Induced Stress in Electrodes during the Coupled Mechano-Electro-Chemical Process," Journal of Power Sources, 342, pp. 896-903.

[13] Rees, G. J., Jolly, D. S., Ning, Z., 2021, "Imaging Sodium Dendrite Growth in all-Solid-State Sodium Batteries using 23Na T2-Weighted Magnetic Resonance Imaging," Angewandte Chemie International Edition, 60(4), pp. 2110-2115.

[14] Bouziane, K., Kehtabi, E. M., Lachat, R., 2020. “Impact of Cyclic Mechanical Compression on the Electrical Contact Resistance between the Gas Diffusion Layer and the Bipolar Plate of a Polymer Electrolyte Membrane Fuel Cell,” Renewable Energy, 153, pp. 349–61.

[15] Mason, T., Millichamp, J., Shearing, P. R., 2013. “A Study of the Effect of Compression on the Performance of Polymer Electrolyte Fuel Cells Using Electrochemical Impedance Spectroscopy and Dimensional Change Analysis,” International Journal of Hydrogen Energy, 38(18), pp. 7414–22.

[16] Renaud, F., Dion, J. L., Chevallier, G., 2011, “A New Identification Method of Viscoelastic Behavior: Application to the Generalized Maxwell Model,” Mechanical Systems and Signal Processing, 25, pp. 991-1010.